sequence alignment program PILEUP[27] and manual adjustment. Phylogenetic analyses were performed using the PHYLIP phylogeny inference package version 3.572. Distance matrices were generated using the DNADIST program with the Jukes–Cantor distance measure. Using *S. castellii* as the outgroup, rooted phylogenetic trees, based on the ITS1 and the *COX2* sequences, were constructed by using the neighbour-joining method[28] and the NEIGHBOR program. We assessed the stability of the individual branches using the bootstrap method[29] with the SEQBOOT, DNADIST, NEIGHBOR and CONSENSE programs.

Received 17 February; accepted 13 March 2000.

1. White, M. *Modes of Speciation* (Freeman, San Francisco, 1978).
2. Naumov, G. Genetic basis for classification and identification of the ascomycetous yeasts. *Stud. Mycol.* **30,** 469–475 (1987).
3. Hunter, N., Chambers, S. R., Louis, E. J. & Borts, R. H. The mismatch repair system contributes to meiotic sterility in an interspecific yeast hybrid. *EMBO J.* **15,** 1726–1733 (1996).
4. Wolfe, K. H. & Schields, D. C. Molecular evidence for an ancient duplication of the entire yeast genome. *Nature* **387,** 708–713 (1997).
5. Seoighe, C. & Wolfe, K. H. Extent of genomic rearrangement after genome duplication in yeast. *Proc. Natl Acad. Sci. USA* **95,** 4447–4452 (1998).
6. Naumov, G., James, S. A., Louis, E. J., Naumova, E. S. & Roberts, I. N. Three new species in the *Saccharomyces* sensu stricto complex: *Saccharomyces cariocanus, Saccharomyces kudriavzevii* and *Saccharomyces mikatae. Int. J. Syst. Bacteriol.* (in the press).
7. James, S. A., Cai, J., Roberts, I. N. & Collins, M. D. A phylogenetic analysis of the genus *Saccharomyces* based on 18S rDNA gene sequences: description of *Saccharomyces kunashirensis* sp. nov. and *Saccharomyces martiniae* sp. nov. *Int. J. Syst. Bacteriol.* **47,** 453–460 (1997).
8. Tamai, Y., Momma, T., Yoshimoto, H. & Kaneko, Y. Co-existence of 2 types of chromosome in the bottom fermenting yeast *Saccharomyces pastorianus. Yeast* **10,** 923–933 (1998).
9. Ryu, S. L., Murooka, Y. & Kaneko, Y. Reciprocal translocation at duplicated RPL2 loci might cause speciation of *Saccharomyces bayanus* and *Saccharomyces cerevisiae. Curr. Genet.* **33,** 345–351 (1998).
10. Ryu, S. L., Murooka, Y. & Kaneko, Y. Genomic reorganization between two sibling yeast species, *Saccharomyces bayanus* and *Saccharomyces cerevisiae. Yeast* **12,** 757–764 (1996).
11. Naumov, G. I., Naumova, E. S., Hagler, A. N., Mendoncahagler, L. C. & Louis, E. J. A new genetically isolated population of the *Saccharomyces* sensu-stricto complex from Brazil. *Antonie Van Leeuwenhoek* **67,** 351–355 (1995).
12. Naumov, G. I., Naumova, E. S. & Louis, E. J. Two new genetically isolated populations of the *Saccharomyces* sensu stricto complex from Japan. *J. Gen. Appl. Microbiol.* **41,** 499–505 (1995).
13. James, S. A., Collins, M. D. & Roberts, I. N. Use of an rRNA internal transcribed spacer region to distinguish phylogenetically closely related species of the genera *Zygosaccharomyces* and *Torulaspora*. *Int. J. Syst. Bacteriol.* **46,** 189–194 (1996).
14. Takezaki, N., Rzhetsky, A. & Nei, M. Phylogenetic test of the molecular clock and linearized tree. *Mol. Biol. Evol.* **12,** 823–833 (1995).
15. Loidl, J., Jin, Q. W. & Jantsch, M. Meiotic pairing and segregation of translocation quadrivalents in yeast. *Chromosoma* **107,** 247–254 (1998).
16. Hani, J. & Feldmann, H. tRNA genes and retroelements in the yeast genome. *Nucleic Acids Res.* **26,** 689–696 (1998).
17. Boeke, J. D., Eichinger, D. J. & Natsoulis, G. Doubling Ty*1* element copy number in *Saccharomyces cerevisiae*: host genome stability and phenotypic effects. *Genetics* **129,** 1043–1052 (1991).
18. Kupiec, M. & Petes, T. D. Meiotic recombination between repeated transposable elements in *Saccharomyces cerevisiae. Mol. Cell. Biol.* **8,** 2942–2954 (1988).
19. Rachidi, N., Barre, P. & Blondin, B. Multiple Ty-mediated chromosomal translocations lead to karyotype changes in a wine strain of *Saccharomyces cerevisiae. Mol. Gen. Genet.* **261,** 841–850 (1999).
20. Codon, A. C., Benitez, T. & Korhola, M. Chromosomal reorganisation during meiosis of *Saccharomyces cerevisiae* baker's yeasts. *Curr. Genet.* **32,** 247–259 (1997).
21. Adams, J. & Oeller, P. W. Structure of evolving populations of *Saccharomyces cerevisiae* adaptive changes are frequently associated with sequence alterations involving mobile elements belonging to the Ty family. *Proc. Natl Acad. Sci. USA* **83,** 7124–7127 (1986).
22. Adams, J., Puskasrozsa, S., Simlar, J. & Wilke, C. M. Adaptation and major chromosomal changes in populations of *Saccharomyces cerevisiae. Curr. Genet.* **22,** 13–19 (1992).
23. Bailis, A. M. & Rothstein, R. A defect in mismatch repair in *Saccharomyces cerevisiae* stimulates ectopic recombination between homologous genes by an excision repair dependent process. *Genetics* **126,** 535–547 (1990).
24. Sniegowski, P., Gerrish, P. & Lenski, R. Evolution of high mutation rates in experimental populations of *Escherichia coli*. *Nature* **387,** 703–705 (1997).
25. Sherman, F., Fink, G. & Hicks, J. *Laboratory Course Manual for Methods in Yeast Genetics* (Cold Spring Harbour Laboratory, Cold Spring Harbour, 1986).
26. Louis, E. J. in *Methods in Microbiology; Yeast Gene Analysis* (eds Truite, M. F. & Brown, A. J. P.) 15–32 (Academic, London, 1998).
27. Feng, D. F. & Doolittle, R. F. Progressive sequence alignment as a prerequisite to correct phylogenetic trees. *J. Mol. Evol.* **35,** 351–360 (1987).
28. Saitou, N. & Nei, M. The neighbor-joining method: a new method for reconstructing phylogenetic trees. *Mol. Biol. Evol.* **4,** 406–425 (1987).
29. Felsenstein, J. Confidence limits on phylogenies: an approach using the bootstrap. *Evolution* **39,** 783–791 (1985).
30. Goddard, M. R. & Burt, A. Recurrent invasion and extinction of a selfish gene. *Proc. Natl Acad. Sci. USA* **96,** 13880–13885 (1999).

**Acknowledgements**

We thank R. Borts and S. Chambers for helpful comments on the manuscript. This work was supported by the Biotechnology and Biological Sciences Research Council and the Wellcome Trust.

Correspondence and requests for materials should be addressed to E.J.L. (e-mail: elouis@molbiol.ox.ac.uk).

# Synaptic activity at calcium-permeable AMPA receptors induces a switch in receptor subtype

**Si-Qiong June Liu & Stuart G. Cull-Candy**

*Department of Pharmacology, University College London, Gower Street, London WC1E 6BT, UK*

**Activity-dependent change in the efficacy of transmission is a basic feature of many excitatory synapses in the central nervous system. The best understood postsynaptic modification involves a change in responsiveness of AMPAR (α-amino-3-hydroxy-5-methyl-4-isoxazole propionic acid receptor)-mediated currents following activation of NMDA (*N*-methyl-D-aspartate) receptors[1,2] or $Ca^{2+}$-permeable AMPARs[3–6]. This process is thought to involve alteration in the number and phosphorylation state of postsynaptic AMPARs[2]. Here we describe a new form of synaptic plasticity—a rapid and lasting change in the subunit composition and $Ca^{2+}$ permeability of AMPARs at cerebellar stellate cell synapses following synaptic activity. AMPARs lacking the edited GluR2 subunit not only exhibit high $Ca^{2+}$ permeability[7] but also are blocked by intracellular polyamines[8–11]. These properties have allowed us to follow directly the involvement of GluR2 subunits in synaptic transmission. Repetitive synaptic activation**

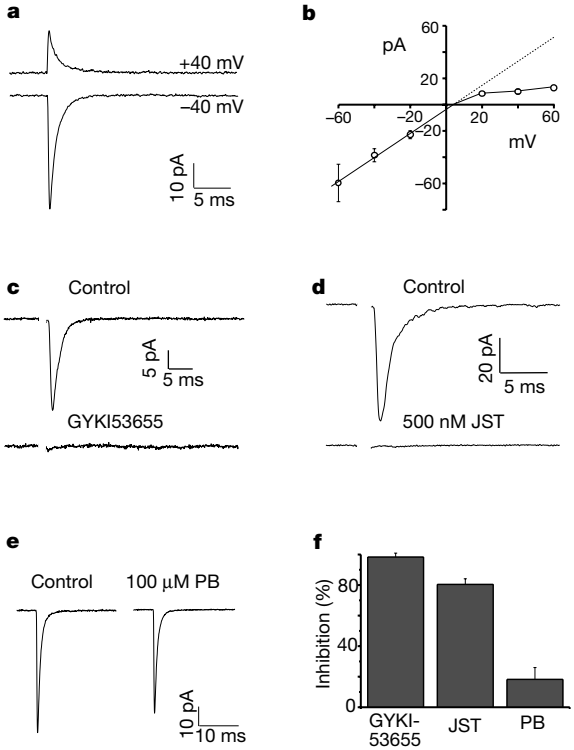


**Figure 1** Synaptic currents in stellate cells exhibit properties of GluR2-lacking AMPARs. **a**, Mean sEPSC at +40 and –40mV, showing reduced current at positive potentials (rectification occurred only when spermine was included in pipette). **b**, Rectifying *I–V* relationship of sEPSCs ($n = 5$). Solid line follows the data points; dashed line at positive potentials represents extrapolated fit for EPSCs behaving ohmically. **c**, Evoked EPSCs (averaged traces) were blocked by the selective AMPAR antagonist GYKI53655 (25 μM). **d**, Joro spider toxin (JST, 500 nM) blocked EPSCs (averaged traces) evoked by threshold stimulation of parallel fibres. **e**, Mean sEPSCs were slightly reduced but not blocked by pentobarbital (PB, 100 μM). **f**, Percentage inhibition of EPSCs by GYKI53655 ($n = 5$), JST ($n = 5$) and PB ($n = 5$; –60 mV). Effect of GYKI53655 and JST was significant ($P < 0.01$).

**of $Ca^{2+}$-permeable AMPARs causes a rapid reduction in $Ca^{2+}$ permeability and a change in the amplitude of excitatory postsynaptic currents, owing to the incorporation of GluR2-containing AMPARs. Our experiments show that activity-induced $Ca^{2+}$ influx through GluR2-lacking AMPARs controls the targeting of GluR2-containing AMPARs, implying the presence of a self-regulating mechanism.**

Minimally evoked parallel fibre input to cerebellar stellate cells is mediated solely by non-NMDA receptors[12]. We found that the selective antagonist GYKI53655 (10–25 μM) reduced the amplitude of evoked excitatory postsynaptic currents (eEPSCs) by 98 ± 3% ($n = 5$; Fig. 1c, f), indicating that these currents are mediated by AMPARs. We have used a number of approaches to determine whether EPSCs and agonist-evoked currents are mediated by the $Ca^{2+}$-permeable variety of AMPARs in these cells. Inclusion of spermine in the pipette solution is known to confer voltage-dependent block on AMPARs lacking GluR2 subunits, which differ from other subunits in being edited in their pore-lining region. This produces a characteristic inwardly rectifying *I–V* relationship[8–11]. The amplitude of spontaneous EPSCs (sEPSCs) (Fig. 1a, b) at the parallel fibre input was reduced at positive membrane potentials. This rectifying *I–V* relationship implies that the EPSCs are mediated mainly by $Ca^{2+}$-permeable AMPARs. We have used various other pharmacological approaches to determine that most synaptic receptors do indeed lack GluR2 subunits.

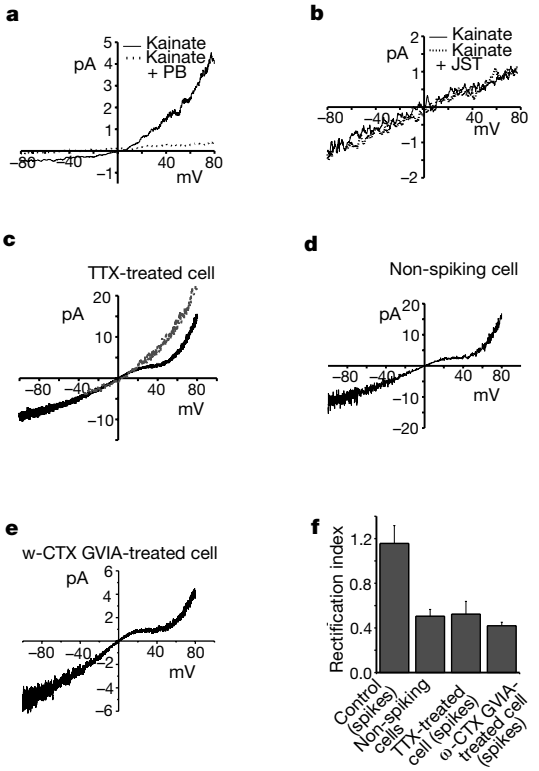


**Figure 2** Extrasynaptic patches exhibit *I–V* plots (outwardly rectifying in **a**; linear in **b**), indicative of GluR2-containing AMPARs. These convert to GluR2-lacking AMPARs in the absence of action potentials, or absence of $Ca^{2+}$ influx through N-type channels. **a**, Kainate-evoked current (solid line) was blocked by pentoparbital (PB, 100 μM; dashed line). **b**, Joro spider toxin (500 nM, thick line) did not inhibit the current. **c**, Inwardly rectifying *I–V* plot after treatment with 500 nM TTX for more than 2 h before recording (thick line); compare this at positive potentials with an averaged control *I–V* plot (thin line). TTX absent during recording. **d**, Inwardly rectifying *I–V* plot in a patch from a cell that did not fire spontaneously action potentials. **e**, Inwardly rectifying *I–V* plot after treatment with 500 nM ω-conotoxin (CTX) GVIA for more than 2 h before recording. **f**, Rectification index was significantly reduced in patches from non-spiking cells ($n = 5$), and cells treated with TTX ($n = 6$) or CTX GVIA ($n = 7$), when compared with control cells ($n = 13$) ($P < 0.03$).

Thus, Joro spider toxin (JST), a subunit-specific blocker of the GluR2-lacking AMPARs[13], reduced the EPSC amplitude by 80 ± 4% ($n = 5$) at –60 mV (Fig. 1d). On the other hand, pentobarbital, which at the concentration used selectively inhibits the GluR2-containing AMPARs[14], reduced the EPSC size by only ~18% ($n = 5$; Fig. 1e, f).

In contrast to the synaptic currents, agonist-evoked currents in somatic outside-out patches exhibited linear or outwardly rectifying *I–V* relationships (Fig. 2a, b) that were blocked by GYKI53655 (90 ± 15%, $n = 5$). This suggests the presence of the $Ca^{2+}$-impermeable variety of AMPARs in the extrasynaptic membrane. Furthermore, pentobarbital reversibly inhibited these currents by 82 ± 13% (at –60 mV; $n = 5$; Fig. 2a), while JST gave only a ~10 ± 15% reduction ($n = 6$; Fig. 2b). These findings indicate that stellate cells express a population of GluR2-containing receptors, but that these occur predominantly extrasynaptically.

To investigate the factors responsible for the selective targeting of GluR2 in these cells, we tested whether synaptic activity could regulate the $Ca^{2+}$ permeability of synaptic AMPARs. After high-frequency synaptic stimulation (300 stimuli at 50 Hz at –60 mV),

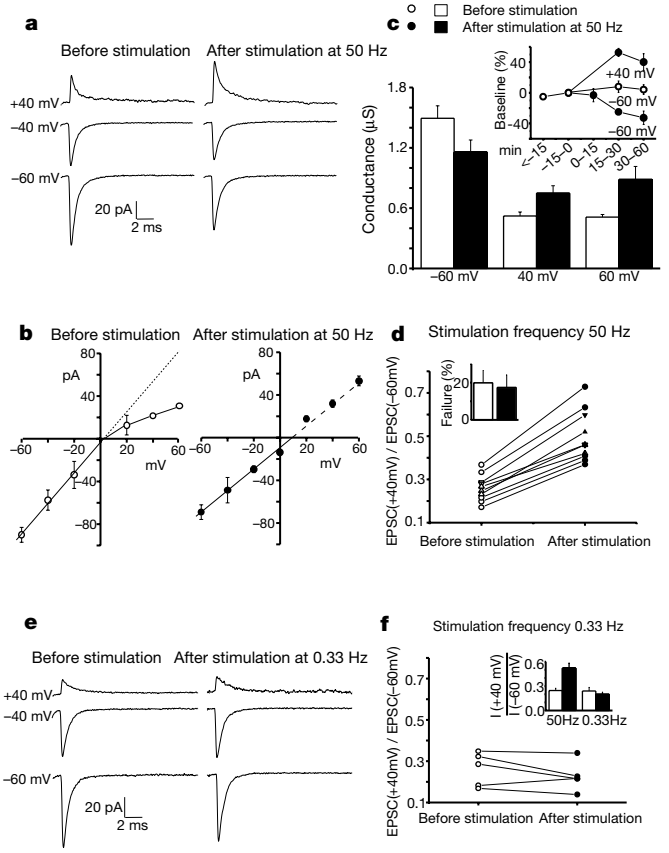


**Figure 3** High-frequency synaptic stimulation induced a change in the rectification of *I–V* relationships of EPSCs. **a**, After high-frequency stimulation (300 stimuli at 50 Hz), EPSC amplitude was reduced at –60mV, but increased at +40 mV. **b**, The inwardly rectifying *I–V* relationship before stimulation (open circles), became linear after 50-Hz stimulation (filled circles) ($n = 9$). Before stimulation the data at positive potentials fell below the line extrapolated from a linear fit; after stimulation data at positive potentials fell along the extrapolated line. **c**, Averaged EPSC conductance values (–60, +40 and +60 mV) changed significantly after stimulation ($P < 0.05$). Inset, stimulation induces a lasting change in EPSC amplitude. **d**, High-frequency stimulation consistently increased the ratio of EPSC amplitudes at +40 mV versus –60 mV but did not change failure rate. Cells were stimulated in the presence of either 120 μM D-AP5/10 μM 7-chlorokynurenic acid (at –60 mV inverted triangle; at –90 mV triangle) or 20 μM D-AP5 (at –60 mV circle; same data set as in **b** and **c**). **e**, **f**, Low-frequency stimulation (300 stimuli at 0.33 Hz) did not alter EPSC amplitude or rectification ($n = 5$). Inset, mean ratio of EPSC amplitude at +40 versus –60 mV increases by more than twofold after high-frequency stimulation at 50 Hz ($P < 0.0005$, paired *t*-test) but remains unchanged after stimulation at 0.33 Hz.

the *I–V* relationship of eEPSCs was changed from predominantly inwardly rectifying (rectification index (RI) = 0.43 ± 0.04, $n = 6$) to a linear form (RI = 1.04 ± 0.14, $n = 6$) (see Figs 3a, b and 4f) within ~15–30 min (Fig. 3c). The EPSC amplitude was significantly decreased at negative potentials (from −93 ± 7 to −65 ± 5 pA at −60 mV; $n = 8$, $P < 0.005$, paired *t*-test) but increased at positive potentials (from 23 ± 2 to 32 ± 4 pA at +40 mV, $n = 6$, $P < 0.02$, paired *t*-test). The decay time constant was little changed (from 0.76 ± 0.04 ms to 0.89 ± 0.08 ms; $n = 11$, $P < 0.05$). The ratio of EPSC amplitudes at +40 mV versus −60 mV increased in all cells examined (without a change in the percentage of failures), regardless of whether cells were held at −60 or −90 mV during stimulation (Fig. 3d). Together, these data indicate an increased expression of the GluR2 subunit at the synapse, which produces a loss of polyamine block and removal of rectification. The reduced EPSC amplitude at −60 mV could reflect changed elementary channel properties as occurs with GluR2-containing recombinant heteroligomers[15]. In contrast, stimulation at a low frequency, with the same number of stimuli (300 stimuli at 0.33 Hz), did not change the EPSC amplitude or the rectification (Fig. 3e, f). Thus, high-frequency stimulation triggers the expression of $Ca^{2+}$-impermeable AMPARs at these synapses. Furthermore, the change was not inhibited by the presence of 120 μM D-AP5 or 10 μM 7-chloro-kynurenic acid (Fig. 3d), indicating that NMDARs were not required for this process. If this activity-dependent change in AMPAR expression is a physiological mechanism then it is expected to be continuously occurring *in vivo*. Hence different amounts of rectification would be seen at different synapses. In keeping with this idea, we found that the ratio of EPSC amplitudes at +40 to those at −60mV ranged from 0.116 to 0.394 in control cells ($n = 42$).

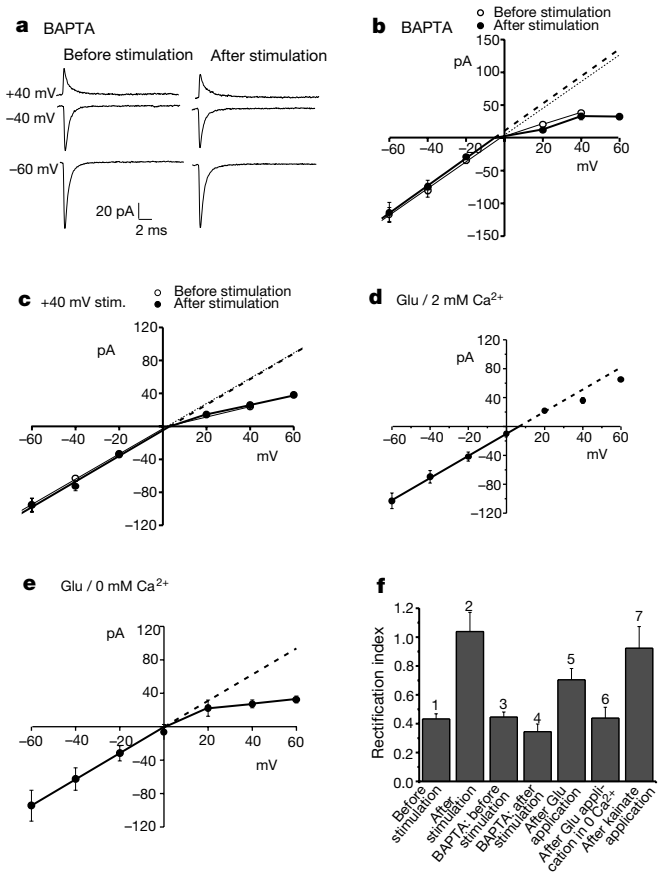


**Figure 4** Calcium influx through non-NMDA glutamate receptors is sufficient to trigger activity-dependent change in EPSC rectification. **a**, **b**, Intracellular BAPTA (20 mM) prevented activity-induced (3 × 100 stimuli at 50 Hz) change in amplitude and inward rectification of EPSCs ($n = 5$). **c**, EPSC amplitude and *I–V* relationship was unaltered if cells were clamped at +40 mV during high-frequency stimulation ($n = 5$). **d**, **e**, EPSCs gave linear *I–V* relationships in cells ($n = 5$) exposed to bath application of 1 mM glutamate. EPSCs remained inwardly rectifying ($n = 5$) if glutamate was applied in $Ca^{2+}$-free solution (plus 3 mM $MgCl_2$). **f**, Summary of rectification index calculated using data in **b**,**d**,**e** and Fig. 3b; *I–V* relationship obtained after bath application of 100 μM kainate and 200–500 nM TTX. Differences between 1 and 2, 1 and 5, 1 and 7, 2 and 4, and 5 and 6 were significant ($P < 0.05$).

We then examined whether the effect of high-frequency synaptic activity could be reproduced by bath application of 1 mM glutamate. After glutamate application, the *I–V* relationship of the EPSC became near linear (for at least 2–3 h) (Fig. 4d). We also found that bath application of 100 μM kainate, which activates non-NMDA receptors but not metabotropic receptors[16], gave rise to EPSCs with linear *I–V* relationships and an RI of 0.92 ± 0.15 ($n = 5$; Fig. 4f). Thus, direct activation of AMPARs can produce an increase in GluR2-containing receptors at this synapse.

To determine whether $Ca^{2+}$ entry was the trigger necessary for activity-dependent targeting of GluR2, we used three different experimental approaches. First, we recorded EPSCs with BAPTA (1,2-bis(*o*-Aminophenoxy)ethane-*N*,*N*,*N*′,*N*′-tetra-acetic acid) (20 mM) included in the pipette to inhibit $Ca^{2+}$ increase in the postsynaptic cell. The high-frequency stimulation no longer altered EPSC amplitude at any of the potentials tested (Fig. 4a,b). Second, cells were held at +40 mV during the period of stimulation, to reduce $Ca^{2+}$ influx through synaptic channels. Again, no change in the EPSC amplitude was observed (Fig. 4c). Third, glutamate was applied in the absence of external $Ca^{2+}$. In these conditions, glutamate failed to produce any change in the inwardly rectifying *I–V* relationship (Fig. 4e), consistent with a requirement for $Ca^{2+}$ entry. Our experiments using high-frequency synaptic stimulation (see above) in cells clamped at −90 mV indicate that a change in GluR2-containing receptors occurs in the absence of activation of voltage-gated $Ca^{2+}$ channels. These data are consistent with the idea that $Ca^{2+}$ influx through the AMPARs is sufficient to produce an intracellular $Ca^{2+}$ rise that causes a rapid change in subunit composition of synaptic receptors.

Does $Ca^{2+}$ entry through voltage-gated $Ca^{2+}$ channels influence the expression of GluR2? Stellate cells fire spontaneous action potentials in the absence of synaptic inputs (mean firing rate ~12 Hz)[17]. We blocked action potential firing (with 500 nM tetrodotoxin (TTX)) for at least two hours, and then examined the agonist-evoked currents in outside-out patches from the soma. The *I–V* relationship was changed from its usual linear or outwardly rectifying form (Fig. 2a, b) to one that showed strong inward rectification (Fig. 2c), consistent with induction of $Ca^{2+}$-permeable extrasynaptic receptors. The rectification index of the patches from TTX-treated cells was reduced to 0.5 (from control levels of ~1.2; see Fig. 2f). Most of the stellate cells fired spontaneous action potentials in the absence of TTX, but some cells in the molecular layer did not (although excitatory and inhibitory synaptic currents were present). Outside-out patches from these cells also exhibited inwardly rectifying *I–V* plots (Fig. 2d), indicative of $Ca^{2+}$-permeable receptors. Furthermore, patches from cells treated with ω-conotoxin GVIA exhibited inwardly rectifying *I–V* relationships (Fig. 2e). These results indicate that local $Ca^{2+}$ influx through N-type $Ca^{2+}$-channel activity during action potentials can influence the normal synthesis or targeting of GluR2 subunits, accounting for the absence of $Ca^{2+}$-permeable extrasynaptic receptors.

Earlier work has shown that $Ca^{2+}$-permeable AMPARs can be differentially localized at some inputs onto hippocampal neurons[18], although the mechanism underlying this differential distribution is unclear. Our experiments indicate that the level of GluR2-containing receptors at the parallel fibre stellate cell synapse, and the soma in these cells, undergoes dynamic changes driven by activity-induced local $Ca^{2+}$influx. The synaptic AMPARs are mostly $Ca^{2+}$ permeable and therefore lack the edited GluR2 subunit. During high-frequency stimulation, increased $Ca^{2+}$ entry through synaptic AMPARs triggers

the insertion of GluR2-containing receptors to the synapse and the removal of GluR2-lacking receptors. This results in a reduced EPSC amplitude at −60 mV, as well as a change in $Ca^{2+}$ permeability. This molecular modification of the receptor would provide self-regulating feedback that further reduces $Ca^{2+}$ entry, and hence limits the level of GluR2-containing receptors. Our finding that GluR2-containing receptors are present in the soma is in keeping with such a mechanism, as local $Ca^{2+}$ influx during action potentials influences GluR2 expression. The presence of GluR2-lacking receptors at synapses, however, may result from attenuation of dendritic invasion by action potentials[19], or from regional differences in $Ca^{2+}$-channel subtype density[20] or $Ca^{2+}$ buffering[21]. Recent studies on CA1 cells have provided evidence for insertion of AMPARs by exocytosis into synaptic regions during long-term potentiation[22,23]. Furthermore, a specific interaction between NSF (*N*-ethylmaleimide-sensitive factor), a protein involved in membrane fusion events, and the carboxy terminus of GluR2 subunits has been described[24–26]. It is therefore feasible that insertion of GluR2-containing receptors, and removal of GluR2-lacking receptors at the synapse, could be mediated by exocytosis and endocytosis, respectively, although redistribution through lateral diffusion cannot be excluded.

Previous observations have shown that neuronal activity can act to regulate EPSC amplitude by changing AMPAR number[23,27–29] and channel properties[30]. Our experiments suggest that synaptic activity can directly determine the subunit composition of a synaptic AMPAR by controlling the expression or targeting of edited subunits. This produces a change not only in amplitude of synaptic currents, but also in their calcium permeability, voltage dependence and facilitation properties[8]. Such a mechanism provides a form of plasticity that is self-regulating, and would represent a significant role for edited non-NMDAR subunits in certain postsynaptic modifications. □

## Methods

### Electrophysiology

Sagittal or coronal cerebellar slices (200–250 μm) were cut with a vibrating microslicer (DTK-1000) from the vermis of 18–20-day-old Sprague–Dawley rats in ice-cold solution (in mM: 125 NaCl, 2.5 KCl, 2 $CaCl_2$, 1 $MgCl_2$, 26 $NaHCO_3$, 1.25 $NaH_2PO_4$, and 25 glucose, saturated with 95% $O_2$ /5% $CO_2$, pH 7.4). Whole-cell patch-clamp and outside-out patch recordings were made with an Axopatch 200A amplifier (Axon Instruments) in external solution which contained $GABA_A$ and NMDA receptor blockers (20 μM bicuculline methobromide, 100 μM picrotoxin and 20 μM D-AP5) at room temperature. A few stimulation protocols, and all agonist application protocols were carried out in a higher concentration of D-AP5 (120 μM) and 7-chlorokynurenic acid (10 μM).

Recordings were made from visually identified neurons located in the outer two-thirds of the molecular layer. Interneurons were usually identified by their ability to fire spontaneous action potentials in the cell-attached configuration and by the presence of spontaneous EPSCs and inhibitory postsynaptic currents in the whole-cell configuration. Electrode resistances were 3–8 MΩ when filled with internal solution (in mM: 95 CsF, 45 CsCl (or 140 $CsMeSO_4$), 10 CsHEPES, 10 CsEGTA, 2 NaCl, 2 ATP-Mg, 1 QX314, 5 TEA, 1 $CaCl_2$, 0.1 spermine, pH 7.3). Series resistance, whole-cell capacitance and input resistance were 12.6 ± 0.7 MΩ, 4.0 ± 0.3 pF ($n = 33$) and 1.28 ± 0.28 GΩ ($n = 16$), respectively. If series resistance was changed by more than 20%, the experiment was discarded. EPSCs were evoked with a patch-electrode containing external solution, by stimulating in the molecular layer (20–100 μs pulses of 5–30 V at 0.33 Hz) and filtered at 10 kHz. Currents from outside-out patches, in response to voltage ramps (42 mV $s^{-1}$), were measured before and during the application of 100 μM kainate or 1 mM glutamate + 100 μM cyclothiazide.

### Synaptic stimulation protocol and application of agonists

Parallel fibres were stimulated at 50 Hz or 0.33 Hz, while the postsynaptic cell was voltage-clamped at −60 mV (unless otherwise indicated). Only when high-frequency stimulation was successful at generating EPSCs, and there was no change in holding current of the postsynaptic cell, was the data used for further analysis. Stimulation strength and duration were kept constant throughout the experiment. Glutamate and kainate were bath applied for ~1–2 min. Synaptic currents were measured between 15 min and 2 h after synaptic stimulation, or after bath application of agonist.

### Analysis

EPSCs were filtered at 4 kHz and digitized at 20 kHz. For the *I–V* analysis, we rejected events that did not have a smooth rise and decay phase. The average at each holding potential was constructed by aligning each event on its point of fastest rise (typically average of 20–40 EPSCs) using N version 4.0 (written by S. Traynelis, Emory University). The mean EPSC amplitudes at negative potentials were fitted by a linear regression. If EPSC amplitude at positive potentials fell below the extrapolated line it was considered an inwardly rectifying *I–V* relationship. The RI of the *I–V* relationship was defined as the ratio of the current amplitude at +40 mV to the predicted linear value at +40 mV (extrapolated from linear fitting of the currents at the negative potentials). The inhibition of the EPSC by GYKI53655 and JST was calculated by integrating the average EPSC before and after drug addition and the average was obtained by aligning all the traces to their stimulus artefact.

The *I–V* plots of agonist-evoked currents in outside-out patches were obtained by subtracting leak current from the current in the presence of kainate or glutamate plus cyclothiazide. The rectification index was defined as the ratio of current amplitude at +40 mV to the predicted linear value at +40 mV (extrapolated from linear fit of the current between −20 mV and +10 mV, as some patches had outwardly rectifying currents). All values are expressed as mean ± s.e.m., except when they are smaller than the size of the symbol. Statistical significance was assessed by the two-tailed Student's *t*-test.

Received 30 November 1999; accepted 20 March 2000.


1. Bliss, T. V. P. & Collingridge, G. L. A synaptic model of memory—long-term potentiation in the hippocampus. *Nature* **361,** 31–39 (1993).
2. Malenka, R. C. & Nicoll, R. A. Long-term potentiation—a decade of progress? *Science* **285,** 1870–1874 (1999).
3. Gu, J. G., Albuquerque, C., Lee, C. J. & MacDermott, A. B. Synaptic strengthening through activation of $Ca^{2+}$-permeable AMPA receptors. *Nature* **381,** 793–796 (1996).
4. Mahanty, N. K. & Sah, P. Calcium-permeable AMPA receptors mediated long-term potentiation in interneurons in the amydala. *Nature* **394,** 683–687 (1998).
5. Feldmeyer, D. *et al.* Neurological dysfunctions in mice expressing different levels of the Q/R site-unedited AMPAR subunit GluR-B. *Nature Neurosci.* **2,** 57–64 (1999).
6. Laezza, F., Doherty, J. J. & Dingledine, R. Long term depression in Hippocampal interneurons: joint requirement for pre- and postsynaptic events. *Science* **285,** 1411–1414 (1999).
7. Geiger, J. R. P. *et al.* Relative abundance of subunit mRNAs determines gating and $Ca^{2+}$ permeability of AMPA receptors in principal neurons and interneurons in rat CNS. *Neuron* **15,** 193–204 (1995).
8. Rozov, A. & Burnashev, N. Polyamine-dependent facilitation of postsynaptic AMPA receptors counteracts paired-pulse depression. *Nature* **401,** 594–598 (1999).
9. Bowie, D. & Mayer, M. Inward rectification of both AMPA and kainate subtype glutamate receptors generated by polyamine-mediated ion-channel block. *Neuron* **15,** 453–462 (1995).
10. Kamboj, S. K., Swanson, G. T. & Cull-Candy, S. G. Intracellular spermine confers rectification on rat calcium-permeable AMPA and kainate receptors. *J. Physiol.* **486,** 297–303 (1995).
11. Koh, D-S., Burnashev, N. & Jonas, P. Block of native $Ca^{2+}$-permeable AMPA receptors in rat brain by intracellular polyamines generates double rectification. *J. Physiol.* **486,** 305–312 (1995).
12. Clark, B. A. & Cull-Candy, S. Frequency-dependent activation of NMDA receptors at an 'AMPA receptor only' synapse in the rat cerebellum. *J. Physiol.* **518P,** 156P (1999).
13. Blaschke, M. *et al.* A single amino acid determined the subunit-specific spider toxin block of α-amino-3-hydroxy-5-methlisoxazole-4-propionate/kainate receptor channels. *Proc. Natl Acad. Sci. USA* **90,** 6528–6532 (1993).
14. Yamkura. T., Sakimura. K., Mishina. M. & Shimoji, K. The sensitivity of AMPA-selective glutamate receptor channels to pentobarbital is determined by a single amino acid residue of the α2 subunit. *FEBS Lett.* **374,** 412–414 (1995).
15. Swanson, G. T., Kamboj, S. K. & Cull-Candy, S. G. Single-channel properties of recombinant AMPA receptors depend on RNA editing, splice variation, and subunit composition. *J. Neurosc.* **17,** 58–69 (1997).
16. Masu, M., Tanabe, Y., Tsuchida, K., Shigemoto, R. & Nakanishi, S. Sequence and expression of a metabotropic glutamate receptor. *Nature* **349,** 760–765 (1991).
17. Hausser, M. & Clark, B. A. Tonic synaptic inhibition modulates neuronal output pattern and spatiotemporal synaptic integration. *Neuron* **19,** 665–678 (1997).
18. Toth, K, & McBain, C. J. Afferent-specific innervation of two distinct AMPA receptor subtypes on single hippocampal interneurons. *Nature Neurosci.* **1,** 572–578 (1998).
19. Spruston, N., Schiller, Y., Stuart, G. & Sakmann, B. Activity-dependent action potential invasion and calcium influx into hippocampal CA1 dendrites. *Science* **268,** 297–300 (1995).
20. Magee, J. Hoffman, D., Colbert, C. & Johnston, D. Electrical and calcium signaling in dendrites of hippocampal pyramidal neurons. *Annu. Rev. Physiol.* **60,** 327–346 (1998).
21. Seidenbecher, C. I. *et al.* Caldendrin, a novel neuronal calcium-binding protein confined to the somato-dendritic compartment. *J. Biol. Chem.* **273,** 21324–21331 (1998).
22. Lledo, P-M., Zhang, X., Sudhof, T. C., Malanka, R. C. & Nicoll, R. A. Postsynaptic membrane fusion and long-term potentiation. *Science* **279,** 399–403 (1998).
23. Shi, S.-H. *et al.* Rapid spine delivery and redistribution of AMPA receptors after synaptic NMDA receptor activation. *Science* **284,** 1811–1816 (1999).
24. Song, I. *et al.* Interaction of the *N*-ethylmaleimide-sensitive factor with AMPA receptors. *Neuron* **21,** 393–400 (1998).
25. Osten, P. *et al.* The AMPA receptor GluR2 C terminus can mediate a reversible, ATP-dependent interaction with NSF and α- and β-SNAPs. *Neuron* **21,** 99–110 (1998).
26. Nishimune, A. *et al.* NSF binding to GluR2 regulates synaptic transmission. *Neuron* **21,** 87–97 (1998).
27. Turrigiano, G. G., Leslie, K. R., Desai, N. S., Rutherford, L. C. & Nelson, S. B. Activity-dependent scaling of quantal amplitude in neocortical ceurons. *Nature* **391,** 892–896 (1998).
28. O'Brien, R. J. *et al.* Activity-dependent modulation of synaptic AMPA receptor accumulation. *Neuron* **21,** 1067–1078 (1998).
29. Carrol, R. C., Lissin, D. V., von Zastrow, M., Nicoll, R. A. & Malenka, R. C. Rapid redistribution of glutamate receptors contributes to long-term depression in hippocampal cultures. *Nature Neurosci.* **2,** 454–460 (1999).
30. Benke, T. A., Luthi, A., Issac, J. T. & Collingridge, G. L. Modulation of AMPA receptor unitary conductance by synaptic activity. *Nature* **393,** 793–797 (1998).



### Acknowledgements

We thank S. Brickley, B. Clark, M. Farrant, C. Misra, S. Traynelis and M. Whim for helpful advice, discussion and comments on the manuscript, and J. Thomas for technical help.

This work was supported by the Wellcome Trust. S.-Q.L. was in receipt of a Wellcome Trust Travelling Fellowship.

Correspondence and requests for materials should be addressed to S.G.C.-C. (e-mail: s.cull-candy@ucl.ac.uk).

# Vagus nerve stimulation attenuates the systemic inflammatory response to endotoxin

**Lyudmila V. Borovikova*, Svetlana Ivanova*, Minghuang Zhang*, Huan Yang*, Galina I. Botchkina*, Linda R. Watkins†, Haichao Wang‡, Naji Abumrad§, John W. Eaton¶ & Kevin J. Tracey§**

** The Picower Institute for Medical Research, Manhasset, New York 11030, USA*
*† Department of Psychology, University of Colorado, Boulder, Colorado 80309, USA*
*‡ Department of Emergency Medicine and § Department of Surgery, North Shore University Hospital, Manhasset, New York 11030, USA*
*¶ Department of Pediatrics, Baylor College of Medicine, Houston, Texas 77030, USA*

**Vertebrates achieve internal homeostasis during infection or injury by balancing the activities of proinflammatory and anti-inflammatory pathways. Endotoxin (lipopolysaccharide), produced by all gram-negative bacteria, activates macrophages to release cytokines that are potentially lethal[1–4]. The central nervous system regulates systemic inflammatory responses to endotoxin through humoral mechanisms[5–8]. Activation of afferent vagus nerve fibres by endotoxin or cytokines stimulates hypothalamic–pituitary–adrenal anti-inflammatory responses[9–11]. However, comparatively little is known about the role of efferent vagus nerve signalling in modulating inflammation. Here, we describe a previously unrecognized, parasympathetic anti-inflammatory pathway by which the brain modulates systemic inflammatory responses to endotoxin. Acetylcholine, the principle vagal neurotransmitter, significantly attenuated the release of cytokines (tumour necrosis factor (TNF), interleukin (IL)-1β, IL-6 and IL-18), but not the anti-inflammatory cytokine IL-10, in lipopolysaccharide-stimulated human macrophage cultures. Direct electrical stimulation of the peripheral vagus nerve *in vivo* during lethal endotoxaemia in rats inhibited TNF synthesis in liver, attenuated peak serum TNF amounts, and prevented the development of shock.**

Vagus nerve signalling is a critical component of the afferent loop that modulates the adrenocorticotropin and fever responses to systemic endotoxaemia and cytokinaemia[12–15]. Efferent vagus nerve signalling may facilitate lymphocyte release from thymus through a nicotinic acetylcholine receptor response[16]. Clinical studies indicate that nicotine administration can be effective for treating some cases of inflammatory bowel disease[17,18], and that proinflammatory cytokines are significantly decreased in the colonic mucosa of smokers with inflammatory bowel disease[19]. Accordingly, we reasoned that the cholinergic parasympathetic nervous system may modulate the systemic inflammatory response.

We established primary human macrophage cultures by incubating human peripheral blood mononuclear cells in the presence of macrophage colony stimulating factor (MCSF). Acetylcholine (ACh) inhibited TNF release dose-dependently in macrophage cultures conditioned by exposure to lipopolysaccharide (LPS) for 4 h (Fig. 1a). We observed a comparable inhibition of TNF release by ACh from macrophages exposed to LPS for 20 h (data not shown), indicating that ACh did not merely delay the onset of the TNF response. We also treated macrophage cultures with carbachol, a cholinergic agonist chemically distinct from ACh, and observed

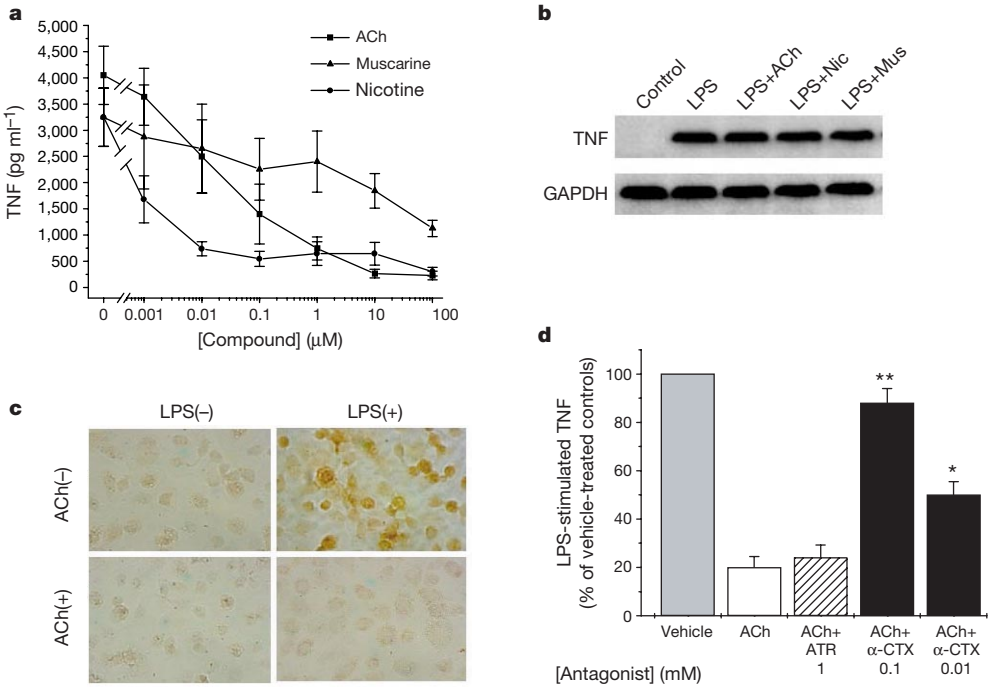


**Figure 1** Cholinergic agonists inhibit LPS-induced TNF synthesis in human macrophage cultures through a post-transcriptional mechanism. **a**, Dose-dependent inhibition of TNF release by ACh (squares), muscarine (triangles) and nicotine (circles) after stimulation with LPS for 4 h. Data are mean ± s.e.m; $n = 9$. **b**, ACh (100 μM), muscarine (100 μM, Mus) and nicotine (100 μM, Nic) do not reduce amount of LPS-stimulated (2 h)TNF mRNA in macrophages. **c**, Immunostaining with anti-TNF antibodies reveals a substantial decrease in LPS-induced (2 h) TNF immunoreactivity in ACh-treated (100 μM) human macrophages. **d**, α-Conotoxin (α-CTX), but not atropine (ATR), restores the LPS-stimulated release of TNF in cultures treated with ACh (10 μM). Neither atropine nor α-conotoxin altered TNF production in vehicle-treated cultures (not shown). Data shown are mean ± s.e.m. of three separate experiments. Asterisk, $P < 0.05$ versus ACh; double asterisk, $P < 0.005$ versus ACh.